A STOCHASTIC MODEL OF PARTICLE DISPERSION IN THE ATMOSPHERE*

B. A. BOUGHTON and J. M. DELAURENTIS

Sandia National Laboratories, P.O. Box 5800, Albuquerque, New Mexico 87185, U.S.A.

and

W. E. DUNN

University of Illinois, Department of Mechanical Engineering, Urbana, Illinois 61801, U.S.A.

Abstract. Stochastic models of turbulent atmospheric dispersion treat either the particle displacement or particle velocity as a continuous time Markov process. An analysis of these processes using stochastic differential equation theory shows that previous particle displacement models have not correctly simulated cases in which the diffusivity is a function of vertical position. A properly formulated Markov displacement model which includes a time-dependent settling velocity, deposition and a method to simulate boundary conditions in which the flux is proportional to the concentration is presented. An estimator to calculate the mean concentration from the particle positions is also introduced. In addition, we demonstrate that for constant coefficients both the velocity and displacement models describe the same random process, but on two different time scales. The stochastic model was verified by comparison with analytical solutions of the atmospheric dispersion problem. The Monte Carlo results are in close agreement with these solutions.

1. Introduction

In recent years, stochastic modeling of atmospheric dispersion has become increasingly popular owing to its simplicity in concept and its applicability to complex problems in which more conventional approaches (e.g., Gaussian plume) cannot be applied. A probabilistic model can easily include buoyancy, droplet evaporation and polydisperse releases. Moreover, treating turbulent dispersion as a stochastic process has a strong intuitive appeal. The stochastic technique is typically implemented in the form of a numerical Monte Carlo model in which a large number of particles are tracked in a Lagrangian frame. A description of the concentration field is then obtained from the particle positions.

Monte Carlo simulations of atmospheric dispersion are based on treating either the particle displacement or the particle velocity as a continuous time Markov process. In the former case, the particle displacements take the form of a random walk. Chandrasekar (1943) considered a very simple random walk in which the step size was held constant and the boundary was either perfectly reflecting or perfectly absorbing, i.e., Brownian motion with barriers. He demonstrated that in the limit of a large number of displacements, the probability density function for this process satisfies the Fickian diffusion equation. This result suggests that solutions to the K-theory advective-

diffusion equation may be obtained using a more general random process. An advantage of this technique, in addition to the capability to include processes that change the particle over its lifetime, is that it is free from the numerical instabilities and diffusion errors that can occur when turbulent dispersion is treated using a conventional Eulerian finite-difference scheme. Anbar (1978) modeled atmospheric diffusion as a superposition of independent Brownian processes. Wippermann (1966) and Runchal et al. (1978) developed more general stochastic processes in an attempt to treat cases where the diffusivity varies with height. It can be shown, however, that these solutions do not satisfy the advective-diffusion equation. Particle settling was not considered and the ground was treated as a reflecting barrier.

Studies which treat the particle velocity as a Markov process assume that the diffusing particles obey a form of Langevin's equation, an equation first used to describe the velocity of a particle exhibiting Brownian motion. In this equation, the force exerted by the fluid on the particle consists of a damping term which is linear in velocity plus a random force independent of the velocity state. Recent investigations using this approach include those of Legg and Raupach (1982), Thomson (1984), and Cogan (1985).

In this paper, the equations governing particle trajectories in a turbulent atmosphere are written as stochastic differential equations. Application of pertinent elements of stochastic differential equation theory provides insight into these models and seems relevant to any analysis that treats turbulent dispersion as a random process. A careful mathematical development of the Markov displacement model using stochastic differential equation theory is given in Section 2. This approach is compared with the Markov velocity or, equivalently, Langevin equation model in Section 3. One notable result is that the two approaches are describing the same random process but are viewing it on two different time scales. In Section 4, a Markov displacement model is developed that extends the applicability of stochastic modeling analysis to cases which have not been addressed in previous studies. The model includes settling as a function of time, boundary behaviors other than perfect reflection and a correct treatment of cases where the diffusivity is a function of vertical position. An estimator is also introduced which uses all of the airborne particle positions to compute the ground-level concentration and deposition. Use of the estimator reduces the number of particles required to produce meaningful ensemble statistics. The simulation is tested by comparison with exact analytical solutions to the dispersion problem in Section 5.

To limit the scope of the problem and to facilitate presentation of results, we shall restrict ourselves to the crosswind-integrated point source problem. This simplification reduces the problem from three to two (x and z) dimensions. The approach described herein can be extended to the three-dimensional case, if desired. Furthermore, we shall assume that turbulent diffusion in the mean wind direction is negligible relative to advection since the turbulence intensity in the mean wind direction is typically much less then the time-averaged mean wind (Haugen, 1973). With this assumption, the equation of particle motion in the x-direction is completely deterministic and will, therefore, not be considered in the development of Section 2.

2. Theoretical Development of the Markov Displacement Model of Turbulent Dispersion

The basis of existing stochastic treatments of turbulent dispersion can be found in the classic investigations of Brownian motion by Einstein and Smoluchowski (see e.g., Fürth, 1956). An accurate description of dispersion in the atmosphere, however, requires significant extension of the simple Brownian theory. The mathematics necessary to simulate atmospheric dispersion are presented below using stochastic differential equation theory. Only turbulent effects in the vertical direction are considered in accordance with our treatment of the crosswind-integrated problem.

In the Markov displacement approach, the particle position $Z(t)$ is given by the stochastic differential equation

$$\frac{\mathrm{d}Z(t)}{\mathrm{d}t} = \mu(Z, t) + \sigma(Z, t)n(t), \quad Z(0) = z_0, \tag{1}$$

where the initial position z_0 is an arbitrary random variable. The function $\mu(Z, t)$ can be identified with deterministic motions. Turbulent effects enter through the second term on the right-hand side of Equation (1). The random function $n(t)$ is white noise, i.e., a stationary, Gaussian random process with a constant spectral density, zero mean, and autocorrelation

$$\langle n(t_1)n(t_2) \rangle = \delta(t_2 - t_1), \quad t_2 > t_1,$$

where $\langle \ \rangle$ denotes an ensemble average over many realizations of the process and δ is the Dirac delta function. White noise is everywhere discontinuous, its integral

$$B(t) = \int_0^t n(t_1)\,\mathrm{d}t_1, \tag{2}$$

however, is continuous but is nowhere differentiable (McKean, 1969). The stochastic process defined by Equation (2), known as the Wiener–Lévy process, is a mathematical model of free particle Brownian motion. It is a nonstationary, Gaussian process with mean zero and independent increments, i.e., for $t_1 < t_2 < t_3$, the random variables $B(t_1), B(t_2) - B(t_1)$, and $B(t_3) - B(t_2)$ are independent.

It is often more convenient to write Equation (1) in terms of $B(t)$ rather than $n(t)$ for analysis purposes. Using Equation (2), we have

$$\mathrm{d}Z(t) = \mu(Z, t)\,\mathrm{d}t + \sigma(Z, t)\,\mathrm{d}B(t), \quad Z(0) = z_0, \tag{3}$$

where $\mathrm{d}B(t)$ is an increment of the Wiener process. If $\mu(Z, t)$ and $\sigma(Z, t)$ satisfy the conditions necessary to guarantee the existence of a unique solution to this equation, $Z(t)$ is a Markov process with continuous sample functions (Arnold, 1974). By definition a Markov process is one in which the probabilities of future states depend only on the present and not on the path by which the present state was achieved. The Markovian

character of Equation (3) is directly attributable to the fact that the Wiener–Lévy process is a process with independent increments. The extensive collection of analytical tools developed for Markov processes can then be used to analyze the solution $Z(t)$.

Equation (3) describes the variation with time of the sample paths $Z(t)$ in a Lagrangian frame. Alternatively, an Eulerian description of the process may be obtained in terms of conditions on the transition probability density $p(z, t, z_0, t_0)$ that a particle released at (z_0, t_0) will be found at z at time t. In our application, the solution $Z(t)$ is a diffusion process (in the mathematical sense) since the functions $\mu(z, t)$ and $\sigma(z, t)$ are continuous with respect to time. Unbounded diffusion processes have the unique property that their transition density is completely determined by the process drift and diffusion parameter which are obtained from only the first two infinitesimal moments. This is a very powerful result in that generally the first two moments are not sufficient to specify a density function uniquely. The drift and diffusion parameter are calculated directly from Equation (3), assuming $Z(t) = z$, as

$$\langle \mathrm{d}Z \rangle / \mathrm{d}t = \mu(z, t)$$

and

$$\langle (\mathrm{d}Z - \langle \mathrm{d}Z \rangle)^2 \rangle / \mathrm{d}t = \sigma^2(z, t) \,,$$

where we have used $\langle \mathrm{d}B \rangle = 0$ and $\langle \mathrm{d}B^2 \rangle = \mathrm{d}t$.

The Eulerian description is based on a partial differential equation that governs the evolution of the transition probability density. For the diffusion process given by Equation (3) with drift $\mu(z, t)$ and diffusion parameter $\sigma^2(z, t)$, we have

$$\frac{\partial}{\partial t} p(z, t, z_0, t_0) + \frac{\partial}{\partial z} [\mu(z, t)p(z, t, z_0, t_0)] -$$

$$-\frac{1}{2} \frac{\partial^2}{\partial z^2} [\sigma^2(z, t)p(z, t, z_0, t_0)] = 0 \,. \qquad (4)$$

Equation (4) is the Fokker–Planck equation for the Markov displacement process and clearly has the same form as the advective-diffusion equation. In the stochastic model, the ensemble mean concentration is calculated from the transition probability density using

$$\langle c(z, t) \rangle = \int\limits_{0}^{t} \int\limits_{0}^{\infty} p(z, t, z_0, t_0)S(z_0, t_0) \, \mathrm{d}z_0 \, \mathrm{d}t_0 \,, \qquad (5)$$

where $S(z_0, t_0)$ is a function describing the known distribution of sources, e.g., $S(z_0, t_0) = Q\delta(z - z_0, t - t_0)$ for an instantaneous point source of strength Q. Applying the integration with respect to z_0 and t_0 to Equation (4), it is straightforward to show that $\langle c(z, t) \rangle$ also satisfies the Fokker–Planck equation.

The advective-diffusion equation for the process we are studying is

$$\frac{\partial}{\partial t} \langle c(z, t) \rangle - w_s(t) \frac{\partial}{\partial z} \langle c(z, t) \rangle = \frac{\partial}{\partial z} \left[K(z, t) \frac{\partial}{\partial z} \langle c(z, t) \rangle \right], \qquad (6)$$

where $w_s(t)$ is the time-dependent settling velocity and $K(z, t)$ is the diffusivity. Comparing this equation with the Fokker–Planck equation shows that the mean concentration obtained from the stochastic process given by Equation (3) will satisfy the advective-diffusion equation if

$$\mu(z, t) = \frac{\partial}{\partial z} K(z, t) - w_s(t) \qquad (7a)$$

and

$$\sigma^2(z, t) = 2K(z, t), \qquad (7b)$$

with the constraint $\partial w_s/\partial z = 0$.

The term $\partial K(z, t)/\partial z$ in Equation (7a) has been neglected in previous models of turbulent dispersion and implies that for cases in which the diffusivity changes with height, there is an effective drift velocity toward larger values of K. This drift arises because the dispersive turbulent motions increase with increasing K and, therefore, particles tend on average to move up $\partial K(z, t)/\partial z$. (This result for the Markov displacement model is analogous to the bias velocity which must be added to a Langevin equation simulation when there is a vertical gradient in the vertical velocity variance (Wilson *et al.*, 1983).) Since the diffusivity increases with height in the lower atmosphere, neglecting the $\partial K(z, t)/\partial z$ term produces an unrealistic accumulation of particles close to the ground. This in turn results in an overestimate of ground-level concentration. The second term in Equation (7a) is simply the deterministic settling velocity.

Equation (3) with $\mu(z, t)$ and $\sigma(z, t)$ as specified in Equation (7) is a means to obtain solutions to the advective-diffusion equation in complex cases not easily treated with conventional Eulerian numerical techniques. Buoyancy effects, evaporation, chemical reaction, and time or space variability in meteorological conditions can all be handled within the Lagrangian framework of our modeling approach.

3. Comparison of the Markov Displacement and Langevin Equation Models

Several studies have used a stochastic model for the particle velocity instead of the particle displacement. Typically the velocity is represented by a Markov process and the position of the particle is determined by integrating the velocity process. Since both models describe similar physical phenomena, it is natural to expect the two approaches to be consistent with one another. However, the integral of the velocity process is not Markov, whereas the displacement model assumes a Markovian character for the particle position. This apparent dilemma can be resolved by observing that both models describe the same random process but on different time scales. We shall demonstrate

this result for the processes with constant coefficients. A rigorous mathematical proof in the more general case involves techniques which are beyond the scope of this paper.

The starting point for the velocity models is a stochastic differential equation developed by Langevin to represent the velocity of a Brownian particle with friction

$$\mathrm{d}W(t) = -\alpha W(t)\,\mathrm{d}t + \lambda\,\mathrm{d}B(t), \quad W(0) = w_0. \tag{8}$$

Here, $W(t)$ is the particle velocity in the vertical direction and the initial velocity w_0 is an arbitrary random variable. In our analysis, $\alpha > 0$ and λ are constants.

With constant coefficients, Equation (8) may be solved using conventional first-order linear differential equation solution techniques,

$$W(t) = \exp(-\alpha t)w_0 + \lambda \int_0^t \exp[-\alpha(t - t_1)]\,\mathrm{d}B(t_1). \tag{9}$$

The moments of $W(t)$ are easily calculated from Equation (9). In particular, evaluation of the variance and covariance shows that $\alpha = \tau_L^{-1}$, where τ_L is the Lagrangian integral time-scale of $W(t)$.

Integrating the velocity we obtain the particle position

$$\tilde{Z}(t) = z_0 + \int_0^t W(t_1)\,\mathrm{d}t_1.$$

If z_0 and w_0 are normally distributed or constant, $\tilde{Z}(t)$ is a Gaussian process, the Ornstein–Uhlenbeck position process.

The result we require may be obtained by comparing the mean and autocorrelation of the Orntein–Uhlenbeck process with the corresponding moments of the Markov displacement process given by Equation (3). Without loss of generality, we shall assume $w_0 = 0$. Then, for the Ornstein–Uhlenbeck process

$$\langle \tilde{Z}(t) \rangle = \langle z_0 \rangle \tag{10a}$$

and

$$\begin{aligned}
\langle \tilde{Z}(t_1)\tilde{Z}(t_2) \rangle = {}& \mathrm{Var}(z_0) + \langle z_0 \rangle^2 + \lambda^2 \min(t_1, t_2)/\alpha^2 + \\
& (\lambda^2/2\alpha^3)\,[2\exp(-\alpha t_1) + 2\exp(-\alpha t_2) - 2 - \\
& \exp(-\alpha|t_1 - t_2|) - \exp(-\alpha(t_1 + t_2))].
\end{aligned} \tag{10b}$$

$\tilde{Z}(t)$ is now completely specified since it is Gaussian and the mean and co-variance are known.

The Markov displacement model analogous to the Ornstein–Uhlenbeck process is obtained from Equation (3) with $\mu(Z, t)$ and $\sigma(Z, t)$ taken as constants. The first two moments of this process are

$$\langle Z(t) \rangle = \langle z_0 \rangle + \mu t \tag{11a}$$

and

$$\langle Z(t_1)Z(t_2) \rangle = \text{Var}(z_0) + \langle z_0 \rangle^2 + \sigma^2 \min(t_1, t_2). \tag{11b}$$

Comparing Equations (10a) and (11a), the means of the two processes are equal if $\mu = 0$, which implies that there is no gravitational settling. The autocorrelation function given in Equation (10b) is considerably more complicated than Equation (11b). However, if in Equation (10b) we let $\alpha \to \infty$ in such a way that λ/α remains constant, we obtain

$$\lim_{\alpha \to \infty} \langle \tilde{Z}(t_1)\tilde{Z}(t_2) \rangle = \text{Var}(z_0) + \langle z_0 \rangle^2 + \lambda^2 \min(t_1, t_2)/\alpha^2,$$

which is identical to Equation (11b) with $\sigma = \lambda/\alpha$. The limiting process is identical to $Z(t)$ defined by Equation (3) with constant coefficients since both processes are Gaussian with the same mean and autocorrelation.

The physical interpretation of the limiting process may be obtained by recalling that $\alpha = \tau_L^{-1}$. So, α is large whenever τ_L is small. In fact, the same limit is obtained whenever τ_L is small compared to the travel time. This implies that Equation (3) with $\mu = 0$ and $\sigma = \lambda/\alpha$ is describing the same process as Equation (8), but for travel times that are larger than the Lagrangian time-scale. This conclusion is consistent with our results which show that the transition density of the process defined by Equation (3) satisfies the advective-diffusion equation and with the travel times over which the gradient transfer hypothesis is valid (Corrsin, 1974). In a similar way, it can be shown that Equation (8) is valid for $t > \tau_a$, where τ_a is the time-scale over which particle accelerations remain correlated. (The models with nonconstant coefficients share the same travel time constraints: the Markov displacement model describes dispersion for $t > \tau_L$ and the Langevin equation model describes dispersion for $t > \tau_a$.)

4. The Monte Carlo Model

This section describes the formulation of a numerical model based on the continuous time Markov process given by Equation (3). As shown in Section 2, the mean concentration obtained from this simulation will satisfy the advective-diffusion equation. A treatment of the boundary condition at the ground and a method to estimate the ensemble mean concentration are also presented.

Using an integer subscript to index time, Equation (3) may be discretized as

$$Z_{i+1} = Z_i + \left[\frac{\partial}{\partial z} K(Z_i, t_i) - w_s(t_i) \right] \Delta t + \sqrt{2K(Z_i, t_i)} r_{i+1}, \tag{12}$$

where we have substituted for $\mu(z, t)$ and $\sigma(z, t)$ from Equation (7) and r_{i+1} is a Gaussian random variable with zero mean and variance Δt.

The equation governing particle movements in the downwind direction x neglecting turbulent diffusion relative to advection is simply

$$X_{i+1} = X_i + \bar{u}(Z_i)\Delta t. \tag{13}$$

The initial conditions are

$$X_0 = 0 \quad \text{at} \quad t_0 = 0$$

and

$$Z_0 = h \quad \text{at} \quad t_0 = 0,$$

for a source located at $x = 0$, $z = h$.

Particle displacements are governed by Equations (12) and (13) for all locations within the semi-infinite domain above the ground. To take into account the removal of airborne material, these movements must be modified as particles interact with the ground. In this context, the term 'ground' is loosely construed to include vegetation and structures which extend above the ground and which affect particle removal. Analytically, the ground is idealized as a smooth flat surface.

Deposition includes the effects of surface roughness, impaction, adsorption and interactions with the vegetative canopy as well as gravitational settling. The various removal mechanisms other than settling are commonly grouped together into a single term in which the rate of removal is assumed to be proportional to the ground-level concentration. Soo and Chen (1982) derived the boundary condition at the ground appropriate for the advective-diffusion equation by extending an analysis of suspension flow in a pipe to the case of a semi-infinite medium. The boundary condition proposed by Soo and Chen may be written

$$K(0, t) \, \partial \langle c(0, t) \rangle / \partial z = [(P_s - 1) w_s(t) + \beta] \langle c(0, t) \rangle,$$

where P_s is the probability that a particle which strikes the ground due to settling is deposited and β is a parameter with units of velocity which corresponds to removal by mechanisms other than settling. In a formulation more commonly applied in atmospheric dispersion, the terms $P_s w_s(t) + \beta$ are combined to form a parameter called the deposition velocity. Thus,

$$K(0, t) \, \partial \langle c(0, t) \rangle / \partial z = [w_d(t) - w_s(t)] \langle c(0, t) \rangle. \tag{14}$$

The boundary condition at the ground locally modifies the transition probability of the Markov process. Previous stochastic models of atmospheric dispersion have had considerable difficulty correctly simulating the boundary condition for cases other than perfect reflection, i.e., $K(0, t) \, \partial \langle c(0, t) \rangle / \partial z + w_s(t) \langle c(0, t) \rangle = 0$. We have devised a straightforward method for handling boundary conditions in which the flux is proportional to the concentration. For concreteness, we shall address the deposition velocity formulation.

Suppose that at the moment t_i the particle is close to the ground and that $\partial K(z, t_i)/\partial z$ is nearly zero in some neighborhood of the ground. For the next short time interval, the particle behaves as if the process had constant drift and variance, i.e., the 'local' process exhibits a drift and variance of approximately $-w_s(t_i)$ and $2K(0, t_i)$, respectively. The probability density for the occurrence of various values of z over a short time is estimated by the solution to the equation (see Equation (4))

$$\frac{\partial}{\partial t} p(z, t, z_i, t_i) = w_s(t_i) \frac{\partial}{\partial z} p(z, t, z_i, t_i) + K(0, t_i) \frac{\partial^2}{\partial z^2} p(z, t, z_i, t_i) \qquad (15a)$$

with the boundary condition

$$K(0, t_i) \frac{\partial}{\partial z} p(0, t, z_i, t_i) = [w_d(t_i) - w_s(t_i)] p(0, t, z_i, t_i) . \qquad (15b)$$

The solution $p(z, t, z_i, t_i)$ to Equation (15) was given by Monin (1959).

The probability that the particle is absorbed during time Δt is the probability that it no longer lies in the interval $[0, \infty)$. This probability is computed from the transition probability density given by Monin as

$$\begin{aligned}
P(z_i, \Delta t) &= 1 - \int_0^\infty p(z, t, z_i, t_i) \, dz \\
&= \phi[-(z_i - w_s \Delta t)/\sqrt{2K\Delta t}] + \\
&\quad w_d/(w_d - w_s) \exp(w_s z_i/K)\phi[-(z_i + w_s \Delta t)/\sqrt{2K\Delta t}] - \\
&\quad (2w_d - w_s)/(w_d - w_s) \exp[w_d z_i/K + w_d(w_d - w_s)\Delta t/K] \times \\
&\quad \phi\{-[z_i + (2w_d - w_s)\Delta t]/\sqrt{2K\Delta t}\} , \qquad (16)
\end{aligned}$$

where $w_s = w_s(t_i)$, $w_d = w_d(t_i)$, $K = K(0, t_i)$ and $\phi(x)$ is the standard Gaussian distribution. Boundary behaviors in which only a fraction of the ground-level particles are absorbed, as well as the extreme cases of perfect reflection and perfect absorption can be simulated with the probability of absorption given in Equation (16). (For perfect absorption, $P(z_i, \Delta t)$ is obtained by taking the limit of Equation (16) as $w_d \to \infty$.) In the model, $P(z_i, \Delta t)$ is used in the following algorithm to simulate the deposition velocity boundary condition.

Above a certain height H, the probability of interaction with the ground is negligible. Whenever a particle is above this threshold, we proceed as if no boundary were present. Now suppose a particle is at a height $z_i < H$ at time t_i. The probability of absorption during time Δt is then $P(z_i, \Delta t)$ as given by Equation (16). In this case, the particle is first moved as if no boundary were present. Then, if a random number from the uniform distribution on $[0, 1]$ is less than $P(z_i, \Delta t)$, the particle is absorbed. Otherwise, we continue the simulation as if the boundary were perfectly reflecting. Specification of the height H is not critical since the probability of absorption falls off very rapidly as the particle moves away from the boundary.

At each time step, the Monte Carlo simulation yields a set of particle positions Z^k, where k indexes particle number. Of primary interest, however, is the mean concentration $\langle c(z, t) \rangle$. Equation (5) shows that to calculate the concentration we must first compute the transition probability density. To estimate $p(z, t, z_0, t_0)$, we employ a nonparametric technique for approximating densities. All of the airborne particles

contribute to the estimate according to their distance from the point z at which the concentration is desired. This reduces the number of particles necessary to obtain reliable ensemble statistics. A Gaussian interpolation function gives the approximation

$$p(z, t, z_0, t_0) \approx p_N(z, t, z_0, t_0) = \frac{1}{N} \sum_{k=1}^{m} \frac{\exp[-(z - Z^k)^2/2\sigma_N^2]}{\sqrt{2\pi}\,\sigma_N\,\phi(z/\sigma_N)} , \qquad (17)$$

where N is the number of particles released, m is the number of particles in the air and the standard deviation σ_N can be related to the moments of the airborne distribution.

The choice of σ_N has a significant effect on the estimate p_N. If σ_N is too large, the approximation suffers from too little resolution. On the other hand, the estimate suffers from too much statistical variation if σ_N is too small. With a limited number of samples, the best one can achieve is some acceptable compromise. An upper bound on $\mathrm{Var}(p_N)$ is

$$\mathrm{Var}(p_N) \leq (N\sigma_N)^{-1} .$$

Therefore, to obtain a small variance, σ_N must decrease to zero slowly enough with N that $N\sigma_N$ approaches infinity. In practice, we have found that $\sigma_N = \sigma_z/N^{1/5}$, where σ_z is the standard deviation of the airborne distribution, works well.

The estimator described above is easily extended to higher dimensions, e.g., a two-dimensional Gaussian interpolation function can be used to include the downwind direction.

5. Verification of the Monte Carlo Model

The proof that the simulation outlined in Section 4 converges to the process whose transition density satisfies the Fokker–Planck equation with the attendant deposition velocity boundary condition is mathematically involved and will not be presented. Instead, the Monte Carlo model is tested by comparison with analytical solutions of the crosswind-integrated point source problem developed by Ermak (1977) and Rounds (1955). The purpose is not to demonstrate the full capability of the model, but to validate the new and unique features of our formulation. Only those cases necessary to verify the model are presented herein. Boughton (1983), in a doctoral dissertation, provides a more extensive set of results including evaporation, comparisons with models commonly used in regulatory applications and comparisons with field measurements.

To minimize the number of parameters required to specify each case, results are presented in terms of the following dimensionless variables: $x_* = xK_r/(\bar{u}_r h^2)$, $z_* = z/h$, $h_* = w_{s,c}h/K_r$, $d_* = h(w_d - w_s)/K_r$, $\bar{u}_* = \bar{u}/\bar{u}_r$, $c_* = \langle c \rangle \bar{u}_r h/Q$, and $j_* = \langle j \rangle \bar{u}_r h^2/(QK_r)$, where j is the local deposition flux, $w_{s,c}$ is a characteristic value of the particle settling velocity and the subscript r indicates a reference value. The parameter h_* relates the turbulence of the atmosphere to the rate of settling and can be thought of as the ratio of the characteristic settling velocity $w_{s,c}$ to the mean turbulent transport velocity K_r/h. For negligible settling velocity (as in the case of a diffusing gas)

or for extremely turbulent atmospheric conditions, h_* approaches zero. Conversely, for large particles or for low turbulence conditions, h_* becomes large. d_* is a measure of the extent to which deposition is enhanced beyond that due to gravitational settling alone. Deposition is increased due to mechanisms other than settling for cases in which $d_* > 0$.

The solution given by Ermak assumes a uniform mean wind and a diffusivity that is a function of downwind distance. In addition, the settling velocity, deposition velocity and diffusivity must all have the same functional dependence on x. This restriction is unrealistic because the settling velocity will either remain constant or decrease with downwind distance, whereas the effective turbulent diffusivity will increase with downwind distance. The solution is particularly useful to us, however for testing the Monte Carlo model's treatment of the deposition velocity boundary condition and our method of estimating the transition probability density from the particle positions. The dimensionless ground-level concentration and deposition flux given by Ermak are shown in the Appendix.

The dependence of the diffusivity on downwind distance must be specified before comparisons with Ermak's solution can be made. Ermak expresses his solution in terms of the Gaussian plume parameter σ_z which is related to the diffusivity by

$$K(x) = (\bar{u}/2)\, d\sigma_z^2/dx .$$

For the cases presented here, the power-law fits of F. B. Smith (see Pasquill and Smith, 1983) will be employed. Thus,
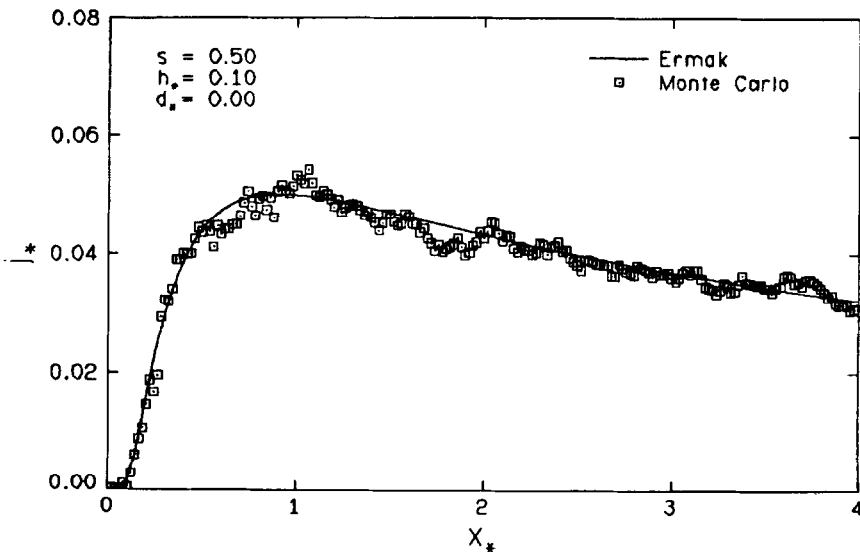
$$\sigma_z = ax^s ,$$

Fig. 1. Comparison of Ermak and Monte Carlo nondimensional deposition flux for the case $s = 0.5$, $h_* = 0.1, d_* = 0$.
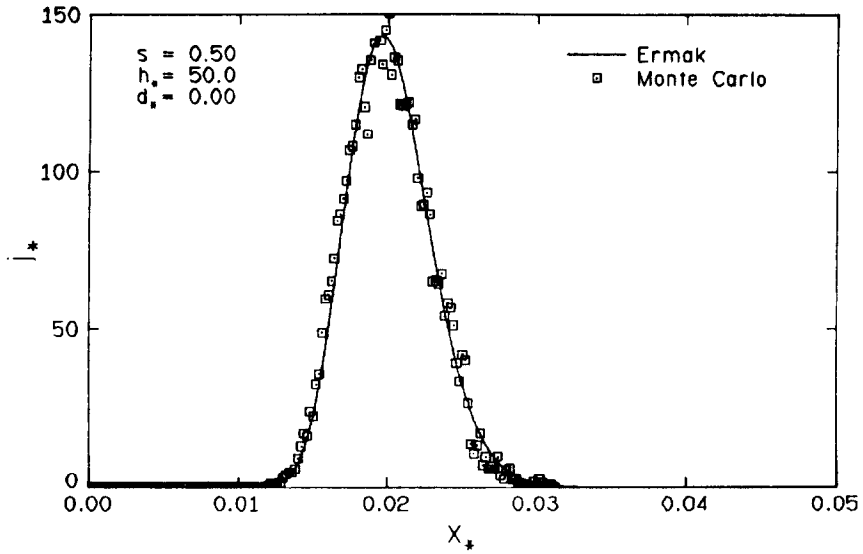
Fig. 2. Comparison of Ermak and Monte Carlo nondimensional deposition flux for the case $s = 0.5$, $h_* = 50$, $d_* = 0$.
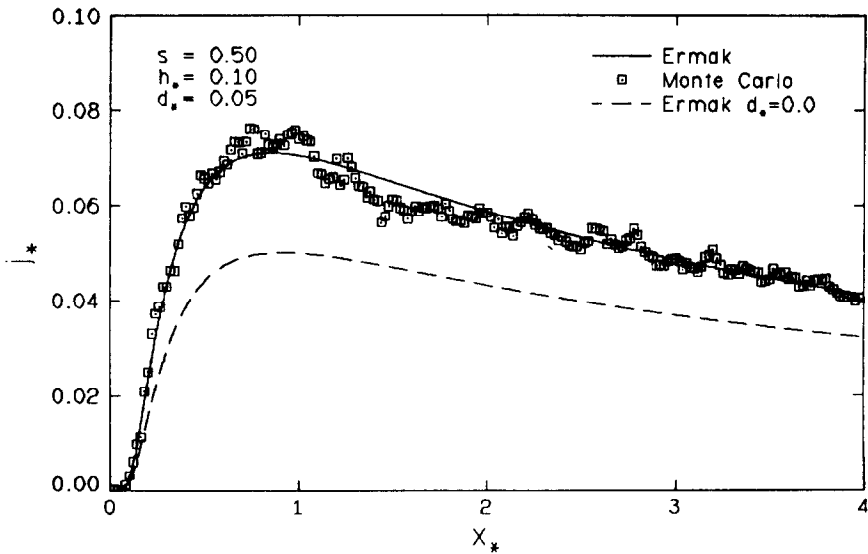

Fig. 3. Comparison of Ermak and Monte Carlo nondimensional deposition flux for the case $s = 0.5$, $h_* = 0.1$, $d_* = 0.05$.

where a and s are constants which depend on surface roughness and atmospheric stability. The case $s = 0.5$ corresponds to a uniform diffusivity, constant settling velocity and constant deposition velocity.

Figures 1 through 5 compare Monte Carlo and Ermak predictions of the dimensionless deposition flux $j_*(x_*)$ for five cases illustrating five basic behaviors:

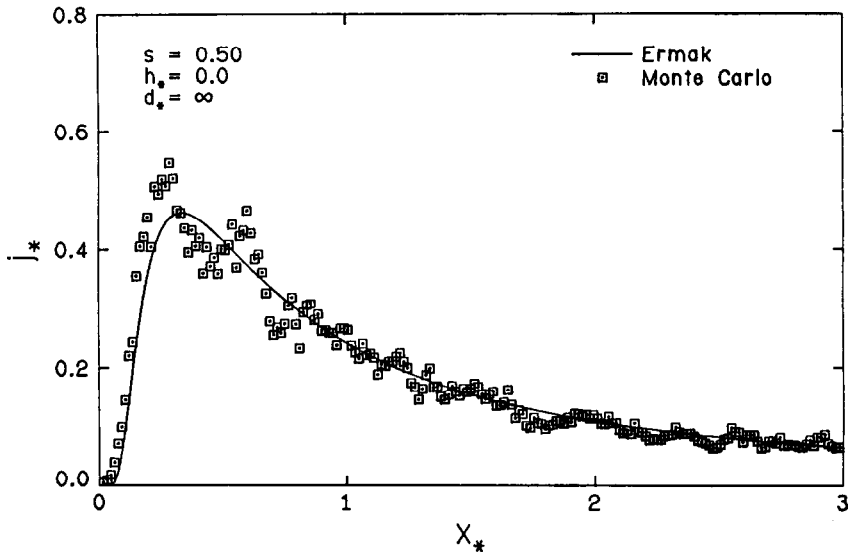(1) Small-h_* ($h_* = 0.1$) with deposition due to gravitational settling only ($d_* = 0$) is shown in Figure 1.

Fig. 4.   Comparison of Ermak and Monte Carlo nondimensional deposition flux for the case $s = 0.5$, $h_* = 0, d_* = \infty$.
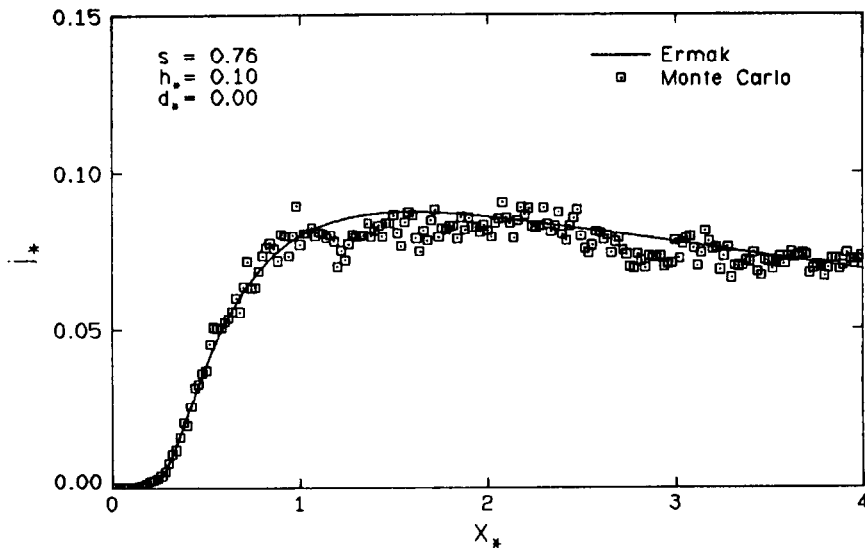

Fig. 5.   Comparison of Ermak and Monte Carlo nondimensional deposition flux for the case $s = 0.76$, $h_* = 0.1, d_* = 0$.

(2) Large-h_* ($h_* = 50$) with deposition due to gravitational settling only ($d_* = 0$) is shown in Figure 2.

(3) Small-h_* ($h_* = 0.1$) with deposition enhanced beyond that due to gravitational settling alone ($d_* = 0.05$) is shown in Figure 3.

(4) Dispersion of a gas or non-settling material ($h_* = 0$) with complete absorption at the ground ($d_* = \infty$) is shown in Figure 4.

(5) Small-h_* ($h_* = 0.1$) with both the settling velocity and diffusivity increasing with downwind distance according to Ermak's constraint is shown in Figure 5.

Agreement between the Monte Carlo predictions and Ermak's exact solution is very good. More extensive testing revealed equally good agreement over a wider range of h_*, d_*, and s. Agreement can be improved further by using more particles. The comparisons shown here using 2000 particles required from 10 to 30 s execution time per case on a Cyber 170.

For cases of constant settling shown in Figures 1, 2, and 3, peak deposition occurs at $x_* = (1 + h_*)^{-1}$ a fact that can be verified analytically. Further investigation indicated that peak deposition occurs close to this point for a wide range of conditions. As shown in Figure 4, the point of peak deposition is shifted upwind in the case of no settling and complete absorption at the ground. In Figure 5, the location of peak deposition is shifted downwind from $x_* = (1 + h_*)^{-1}$ due to the relatively smaller settling velocity close to the source.

Figures 1 and 3 illustrate the deposition behavior typical of small-h_* cases; a rapid rise to a peak followed by a long, slowly decreasing tail. Small-h_* values indicate that the dispersion is dominated by turbulence effects rather than gravitational settling. The deposition pattern shows a peak close to the source due to turbulent motions rapidly
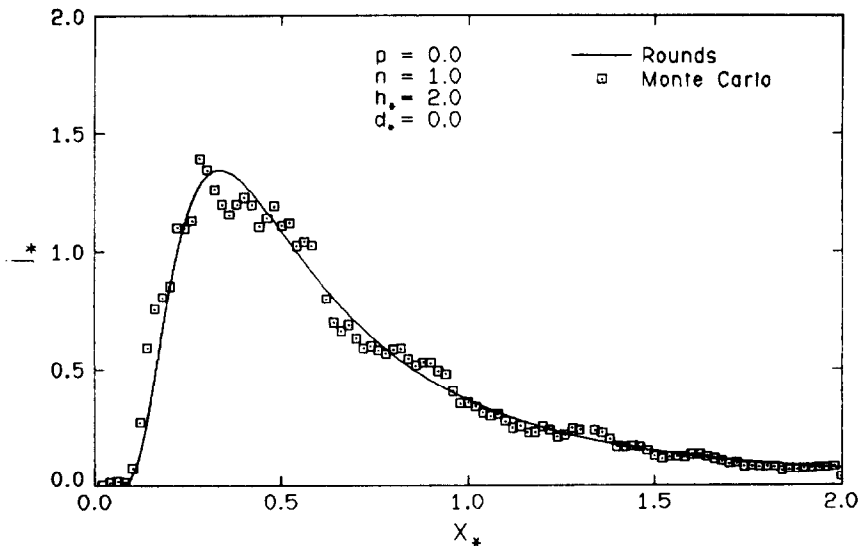

Fig. 6.   Comparison of Rounds and Monte Carlo nondimensional deposition flux for the case $p = 0, n = 1$, $h_* = 2$.

bringing the particles down close to the ground. As h_* becomes large, the behavior is increasingly deterministic and the deposition flux j_* becomes more peaked and symmetric about the point $x_* = (1 + h_*)^{-1}$ as shown in Figure 2.

If processes other than gravitational settling contribute to deposition, the deposition rate increases at downwind distances close to the source. This effect is illustrated in Figure 3 wherein $d_* = h_*/2 = 0.05$ produces an increase of roughly 30% in peak deposition.

Rounds' solution assumes that the mean wind and diffusivity vary as power laws in z. In terms of the dimensionless variables, we have $\bar{u}_* = z^p$ and $K_* = z_*^n$. The solution includes settling when the diffusivity grows linearly in z_* ($n = 1$) and provides a test of our treatment of cases in which $\partial K/\partial z$ is not zero. The solution given by Rounds is shown in the Appendix.

The Monte Carlo predictions are compared to Rounds' solution in Figures 6 and 7. These results illustrate the model's capability to handle cases with wind shear, gravitational settling, deposition and a diffusivity that is a function of height. Again, we see that peak deposition occurs close to the point $x_* = (1 + h_*)^{-1}$. Wind shear shifts the location of peak deposition upwind and increases the maximum value. Both these effects are attributable to the decrease in wind speed as a particle approaches the ground.
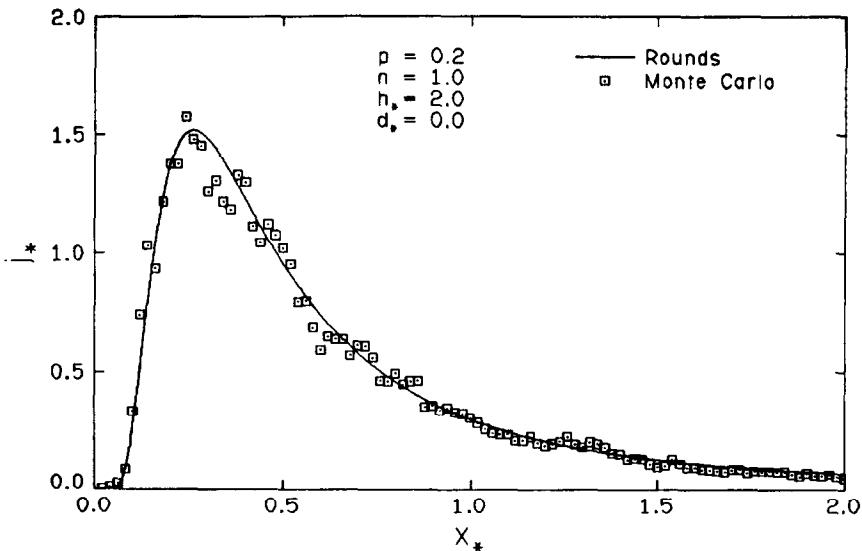

Fig. 7. Comparison of Rounds and Monte Carlo nondimensional deposition flux for the case $p = 0.2$, $n = 1$, $h_* = 2$.

6. Conclusion

The mathematical theory underlying models which treat atmospheric dispersion as a random process has been investigated using stochastic differential equation theory. This

analysis shows that previous Markov displacement models have neglected a term involving the derivative of the diffusivity with respect to height. In addition, we have demonstrated that for constant coefficients, the Markov displacement and Langevin equation models both describe the same random process but on different travel times. A Markov displacement model was subsequently developed which includes settling, deposition and a method of handling any boundary condition in which the flux is proportional to the concentration. An estimator of the transition probability density was also introduced in which all the airborne particles contribute to the concentration at any given location, thereby reducing the number of particles required to produce meaningful ensemble statistics.

Inasmuch as the predictions of the Monte Carlo model are in close agreement with exact solutions, we believe the results presented here represent a significant improvement in the treatment of the boundary, in estimating the ensemble mean concentration and in simulating cases with particle settling. The techniques developed here can be carried over to extend the applicability of Langevin equation models.

Acknowledgements

Appendix. Dimensionless Ground-Level Concentration and Deposition Flux Formulas as Given by Ermak and Rounds

Ermak (1977)

   Concentration:

$$c_*(x_*, 0) = (\sqrt{2/\pi}/\sigma_{z*}) \exp[-(\xi - 1)^2/2\sigma_{z*}^2] - [d_*/K_* + \xi/\sigma_{z*}^2] \times$$
$$\times \exp\{2\xi/\sigma_{z*}^2 + (d_*/K_*)[1 + \xi + (d_*/K_*)\sigma_{z*}^2/2]\} \times$$
$$\times \operatorname{erfc}\{[1 + \xi + (d_*/K_*)\sigma_{z*}^2]/\sqrt{2}\sigma_{z*}\},$$

where $\xi = (w_{s*}/K_*)(h_* \sigma_{z*}^2/2)$.
   Deposition:

$$j_*(x_*) = (d_* + h_* w_{s*})c_*(x_*, 0).$$

Rounds (1955)

   Concentration:

$$c_*(x_*, 0) = \alpha \exp[-(\alpha^2 x_*)^{-1}]/[(\alpha^2 x_*)^{1-v}\Gamma(1-v)],$$

where $\bar{u}_* = z_*^p$, $K_* = z_*^n$ and $\alpha = 2 + p - n$. For $h_* = 0$, $v = (1-n)/\alpha$. For $h_* \neq 0$ and $n = 1$, $v = -h_*/\alpha$.

Deposition:

$$j_*(x_*) = h_* c_*(x_*, 0).$$

References

Anbar, D.: 1978, 'A Diffusion Model for Use With Directional Samplers', *Atmos. Envir.* **12**, 2131–2138.

Arnold, L.: 1974, *Stochastic Differential Equations: Theory and Applications*, John Wiley and Sons, New York.

Boughton, B. A.: 1983, 'Turbulent Atmospheric Transport and Deposition of Particles with Settling and Evaporation', Ph.D. Thesis, University of Illinois, Urbana, Illinois.

Chandrasekar, S.: 1943, 'Stochastic Problems in Physics and Astronomy', *Rev. Modern Phys.* **15**, 1–98.

Cogan, J. L.: 1985, 'Monte Carlo Simulation of Buoyant Dispersion', *Atmos. Envir.* **19**, 867–878.

Corrsin, S.: 1974, 'Limitations of Gradient Transport Models in Random Walks and in Turbulence', *Adv. Geophys.* **18A**, 25–60.

Ermak, D. L.: 1977, 'An Analytical Model for Air Pollutant Transport and Deposition From a Point Source', *Atmos. Envir.* **11**, 231–237.

Fürth, R. (ed.): 1956, *Investigations on the Theory of Brownian Movement*, Dover Publications, Inc., New York.

Haugen, D. A. (ed.): 1973, *Workshop on Micrometeorology*, American Meteorological Society, Boston, MA.

Legg, R. P. and Raupach, M. R.: 1982, 'Markov-Chain Simulation of Particle Dispersion in Inhomogeneous Flows: the Mean Drift Velocity Induced by a Gradient in Eulerian Velocity Variance', *Boundary-Layer Meteorol.* **24**, 3–13.

McKean, H. P.: 1969, *Stochastic Integrals*, Academic Press, New York.

Monin, A. S.: 1959, 'On the Boundary Condition on the Earth Surface for Diffusing Pollution', *Adv. Geophys.* **6**, 435–436.

Pasquill, F. and Smith, F. B.: 1983, *Atmospheric Diffusion*, third edition, Ellis Horwood Limited, England.

Rounds, W.: 1955, 'Solutions of the Two-Dimensional Diffusion Equation', *Trans. Amer. Geophys. Union* **36**, 395–405.

Runchal, A. K., Bealer, A. W., and Segal, G. S.: 1978, *A Completely Lagrangian Random-Walk Model for Atmospheric Dispersion*, Proc. of the Thirteenth Symp. on Atmos. Poll., Paris, April 26–28.

Soo, S. L. and Chen, F. F.: 1982, 'The Boundary Condition of the Diffusion Equation', *Powder Tech.* **31**, 117–119.

Thomson, D. J.: 1984, 'Random Walk Modeling of Diffusion in Inhomogeneous Turbulence', *Quart. J. Roy. Meteorol. Soc.* **110**, 1107–1120.

Wilson, J. D., Legg, B. J., and Thomson, D. J.: 1983, 'Calculation of Particle Trajectories in the Presence of a Gradient in Turbulent-Velocity Variance', *Boundary-Layer Meteorol.* **27**, 163–169.

Wippermann, F. K.: 1966, 'On Turbulent Diffusion in an Arbitrarily Stratified Atmosphere', *J. Appl. Meteorol.* **5**, 640–645.